International Journal of Heat and Mass Transfer 137 (2019) 1041–1052

Contents lists available at ScienceDirect

International Journal of Heat and Mass Transfer

journal homepage: www.elsevier.com/locate/ijhmt

Influence of fin height on heat transfer and fluid flow characteristics of rectangular microchannel heat sink

Yogesh K. Prajapati

Department of Mechanical Engineering, National Institute of Technology Uttarakhand, Srinagar (Garhwal), Uttarakhand 246174, India

ARTICLE INFO

Article history:
Received 2 February 2019
Received in revised form 23 March 2019
Accepted 3 April 2019
Available online 6 April 2019

Keywords:
Heat transfer
Open microchannel
Single phase flow
Varying fin height
Heat flux

ABSTRACT

Heat transfer and fluid flow behavior have been studied numerically in rectangular parallel microchannel heat sinks with varying fin height. Seven different cases have been considered by varying the fin heights from 0.4 to 1.0 mm. Completely closed heat sink (conventional configuration) of 1.0 mm fin height is one of the cases while remaining six heat sink configurations hold open space between fin top surfaces and cover wall. Three dimensional (3D) numerical simulations were carried out for the range of operating parameters where heat flux varied from 100 to 500 kW/m^2 and Reynolds number from 100 to 400. Single phase liquid water flows as coolant in the heat sink to remove heat. Optimization of fin height has been done to achieve maximum heat transfer rate and overall thermal performance of the heat sink. It has been observed that proposed design of the heat sinks facilitate distinct heat dissipation capacity and fluid flow characteristics. Predicted results i.e. temperature distribution, heat transfer coefficient pressure drop and velocity profile clearly reveal that heat transfer increases with increasing fin height however, heat sinks of considerably shorter fin heights (0.4 – 0.6 mm) have less potential to transfer heat. Pressure drop also increases with fin height because flow obstruction rises. It has been found that heat sink of fin height 0.8 mm exhibits maximum heat transfer which is even higher than fin heights of 0.9 mm and 1.0 mm (completely closed heat sink). Net convective surface area and typical flow behavior caused by available open space have been identified as major reasons to influence the overall thermal performance of the proposed heat sinks.

1. Introduction

Heat transfer enhancement is essentially required in various applications including heat exchangers, compact heat sinks used for electronic cooling and many more. In the current era, due to rapid digitalization followed by compact and miniaturized devices, heat generation per unit volume has significantly increased. Consequently, challenges have been elevated to remove considerable amount of heat from a limited space so that safe use and long life of device could be insured. Since last three decades, enormous research works have been carried out with aim to improve the heat transfer rate and thermal performance of microchannel heat sink. Heat dissipation from microchannel heat sink may be increased through different ways [1–3,5–9] i.e. geometrical modification, coolant type and its flow characteristics, via single phase or flow boiling cooling, morphology of channel surface etc. Although phase change (flow boiling) of coolant ensures higher heat transfer [1,2] along with other advantages, it causes some undesirable phenomenon such as severe instabilities, high pressure drop and complex flow behavior which limit the application of two-phase flow boiling in microchannels. Compared to flow boiling of coolant, single-phase cooling is well understood and established in heat transfer applications and it has been consistently emphasized in the research community. Moreover, researchers are putting efforts to further improve the thermal performance of microchannel heat sink with single phase coolant flow [3]. Among the various suggested techniques to enhance heat transfer, geometrical modifications along with coolant type i.e. nanofluid and others have been found prominent [4]. Even after enormous geometrical amendments, rectangular parallel channel profile has been most commonly examined and found suitable [2,5] for heat sink application due to its simple design, ease of manufacturing, elementary flow characteristic and less pressure drop. It should be note that rectangular parallel profile of microchannel has received considerable attention and also secured its commercial applications in compact heat sink. Therefore, it is desirable to incorporate appropriate modifications by benchmarking rectangular parallel profile.

Wang et al. [5] compared the heat transfer performance of three configurations i.e. rectangular, triangular and trapezoidal shaped

E-mail address: yogesh.k@nituk.ac.in

https://doi.org/10.1016/j.ijheatmasstransfer.2019.04.012
0017-9310/

Nomenclature

A	area, mm^2
A_c	cross-section area, mm^2
c_p	specific heat, J/kg K
D_h	hydraulic diameter, mm
H	heat sink height, mm
h	heat transfer coefficient, W/m^2 K
k	thermal conductivity, W/m K
L	heat sink length, mm
Nu	Nesselt number
p	pressure, Pa
P	perimeter mm
q	heat flux, kW/m^2
Re	Reynolds number
T	temperature, K
V	velocity, m/s
W	heat sink width, mm

Greek symbols

ρ	density, kg/m^3
μ	viscosity, Pa·s

Subscript

b	bottom
c	channel
$conv$	convective
f	fin
in	inlet
l	liquid
out	outlet
w	wall

microchannel. It was found that geometry and channel shape have the notable influence on coolant flow behavior and overall heat transfer performance. For the considered range of hydraulic diameter and aspect ratio (range of 8.904–11.442), rectangular configuration has the lowest thermal resistance and better heat transfer performance compared to other two channel profiles. In order to reduce pressure drop and thermal resistance, Lu et al. [6] proposed the wavy microchnnel with porous fins. Porosity effect provides the favorable flow condition that helps to minimize the pressure drop along with thermal resistance. Li et al. [7] numerically studied the combined effect of triangular cavities and rectangular ribs on overall performance of microchannel heat sink. Study reveals that interrupted flow, redevelopment of thermal boundary layer and extensive mixing of the fluid accelerate the heat transfer enhancement. Similarly, Beng and Japar [8] found the better thermal performance of triangular cavities compared to straight channel. Oblique or segmented fin profile has been one of the modifications made by several researchers [9–12]. Interconnecting flow passage of the oblique fins helps to originate secondary flow, enhance fluid mixing and temperature uniformity in the substrate. Such profile expedites re-initializing thermal boundary layer at the edges of fins that result in increased heat transfer at comparable pressure loss [11,12]. Wavy and serpentine designs of the channels have also been extensively studied in the literature to achieve favorable flow conditions and high heat transfer rate [13,14]. In order to further increase the performance; recently Ghani et al. [15] proposed sinusoidal cavities and rectangular ribs at the side wall of the channel. Better performance was achieved as a result of large flow area and disturbed flow. In the consequent work, Ghani et al. [16] numerically studies interconnecting type channel with rectangular rib. It was found that in addition to increased flow area, existing rib pushes coolant to pass through the secondary flow passages that result in flow mixing and increased heat transfer. Huang et al. [17] introduced the jet and dimple arrangements. Different shape dimples are placed in the channel and over which jet impinges. Convex dimples were found to perform best cooling effect compared to concave and mixed dimples structures. Offset ribs on side walls of microchannels also help to improve the heat transfer. Comparing the different shaped ribs, Chai et al. [18,19] concluded that at lower value of *Re* forward triangular rib whereas at higher *Re* semicircular offset ribs are showing good performance nevertheless, offset rib configuration suffer significantly high pressure drop with increasing *Re*. Comparative performance analysis by Huang et al. [20] of slotted microchannles with three different configuration i.e. rectangular, staggered rectangular and trapezoidal staggered show that trapezoidal staggered has the better thermal performance. Hence authors have suggested that staggered channel profile may be a better choice over parallel flow channels.

Microchannel heat sinks with pin fin arrangements have received considerable attention these days by several authors. Yeom et al. [21] experimentally investigated the micro-pin fin array with air as cooling medium. Authors have pointed out that more numbers of fins results in higher surface area however, major cause of increased heat transfer is due to distinct fluid flow nature around the pin fin. Yang et al. [22] compared the five different patterns of pin-fin heat sinks. Different shapes of the pin-fins have distinct thermo-fluid behavior that causes varying thermal resistance and pressure drop trend. Hexagonal cross-section fin was found to have lowest thermal resistance. Yadav et al. [23] numerically investigated the single row of rectangular microchannel in which cylindrical pin-fins are placed in different arrangements. Upstream arrangement of the pin-fin has the good cooling performance compared to remaining configurations. Moreover, it has been pointed out that pin-fins increases the surface area and also disrupt the flow and thermal boundary layer that favour the heat transfer enhancement. Number of pin-fins or fin porosity and its located angle also influence the cooling performance of heat sink. The optimum values of these factors for square pin-fins attributed to better heat transfer compared to circular pin-fins [24]. Recently, Rasouli et al. [25] investigated the diamond shaped micro pin-fin heat sink with varying eight numbers of pitch and aspect ratios. Vortex shedding was observed at some specific configurations and below some specified range of pitch and aspect ratio. Chiu et al. [26] also observed the effect of micro pin-fin porosity and fin diameter on heat transfer performance of the heat sink. Yang et al. [27] optimized the structural design and operating parameters of pin-fin microchannel using uniform design model. It was emphasized that uniform design model could be better alternate for experimental design. Total thermal resistance is an important factor that needs to be reduced to ensure better cooling performance of microchannels.

Zhai et al. [28] suggested that thermal resistances of the heat sink especially, convective thermal resistance needs to be reduced which would play a vital role for heat transfer enhancement in microchannel. Furthermore, uniform flow distribution should be sustained by appropriate design of entrance region so that temperature uniformity would be maintained. In a recent review article Ghani et al. [29] comprehensively covered the geometrical

modifications that have been furnished to achieve the high performance of microchannel heat sink. Authors have pointed out that despite numerous sincere efforts for increasing the heat transfer in microchannel heat sinks a robust design is far from development.

Although several studies have been undertaken on microchannel heat sink however, in order to achieve the increasing cooling challenges of miniature electronic devices, consistent research works are essentially required to enhance the heat transfer rate and overall thermal performance. Based on the above literature survey and to author's best knowledge, the influence of fin height in microchannel heat sink is seldom investigated in the literature. Therefore, in the present work, rectangular parallel microchannel is studies where height of the fins has been varied. Fin height variation evolves an open type microchannel configuration. Parametric study has been accomplished to identify the most appropriate fin height which provides maximum heat transfer performance for the given configuration of the microchannel heat sinks. Moreover, it is anticipated that proposed design will also secures several other advantages over completely closed conventional microchannels.

2. Geometry and numerical approach

Fig. 1 shows the schematic and isometric view of the open microchannel heat sink. Unlike completely closed microchannels where coolant is restricted to flow only through channel passages, in the present geometry, coolant may flow in the channel and also through the open space available between top cover wall and fin top surface as shown in Fig. 1(a). It is worth mentioning that shorter fin height creates the open space, smaller the fin height more open space would be available at the top. Such design of the microchannel heat sink may be considered as open channel heat sink. It modifies the flow passages and hence coolant flow behavior inside the channel readjusts accordingly. Subsequently, in addition to the confined channel flow, fluid also comes in contact with the top surface of the fins and exposed to the open space. It holds the several advantages compared to completely closed heat sinks. (a) As it holds open space above the fin top, uniform coolant distribution in all channels at the channel entrance is not a concern (b) requires less material for fabrication, (c) lighter in weight and (d) easy to assemble as no need to prevent inter-channel coolant flow. Moreover, it deserves various applications and may be used as a substitution of the closed microchannel in the compact heat sink, MEMS, microelectronics, biomedical and chemical industries.

In the present work, three dimensional (3D) numerical investigations of open rectangular microchannel heat sink have been carried out. Geometry of the heat sink having fin height 0.4 mm (causing maximum open space available) has been shown in Fig. 1(a). Heat sink consists of four channels and three fins. Coolant flow is confined between the two side walls. As discussed above, height of the fin has been varied accordingly; total seven geometries of different fin heights (0.4, 0.5, 0.6, 0.7, 0.8, 0.9 and 1.0 mm) have been considered. Fin height of 1.0 mm represents the completely closed conventional microchannel without any open space. This is the most popular and conventional choice of microchannel heat sink design. This configuration has been examined for comparison of the results. Hence, it should be noted that total seven cases have been thoroughly analyzed and discussed in the current study. Total height of the heat sink is 1.1 mm, which includes bottom wall thickness of 0.1 mm. Total length of the heat sink is 15 mm in which fin length is 13 mm since they have been made-up after 2 mm from the inlet as shown in Fig. 1(b). It attributes to avoid the multiple inlets and ensures that an organized flow interact with the leading edge of the channels and fins. Towards the outlet side, fins are extended up to outlet of the heat sink. Total width of the heat sink is 3.7 mm which includes side walls of thickness 0.1 mm each. Width of each fin and channel is fixed to 0.5 mm. Comprehensive dimensions of the heat sink geometry have been listed in Table 1.

Table 1
Geometrical configuration of the heat sink.

Parameter	Value (mm)
Heat sink width (W)	3.7
Height of heat sink ($H = H_c + H_b$)	1.1
Bottom wall thickness (H_b)	0.1
Side wall width (W_w)	0.1
Channel width (W_c)	0.5
Fin width (W_f)	0.5
Fin height (H_f)	0.4–1
Heat sink length (L)	15

2.1. Governing equation

Single phase liquid water has been considered as a cooling medium. In order to solve the conduction heat transfer in solid section and convection heat transfer in fluid zone along with solid-fluid interface, conjugate technique has been implemented in the commercially available software ANSYS FLUENT version 18.0. Several researchers [5,7,15–17] have used this method to solve similar type of problems and certainly accurate results have been predicted. Steady state simulations have been performed for the single phase flow of the liquid coolant. Numerical simulation has been executed considering the following assumptions:

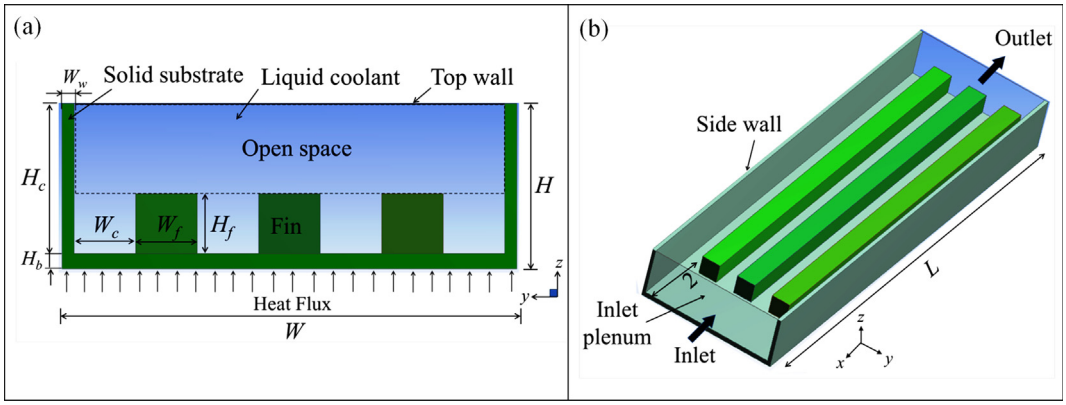

Fig. 1. (a) Schematic and (b) Isometric view of computational domain.

(i) incompressible fluid
(ii) steady and laminar flow
(iii) copper substrate holds constant thermal conductivity
(iv) outer walls are insulated

Considering the above assumptions and based on conservation of mass (continuity), momentum and energy, following governing equations have been solved for fluid and solid region.

Continuity equation

$$\nabla \cdot \vec{V} = 0 \tag{1}$$

momentum equation can be simplified to

$$\rho_l\left(\vec{V} \cdot \nabla \vec{V}\right) = -\nabla P + \nabla \cdot (\mu_l \nabla \vec{V}) \tag{2}$$

for liquid coolant, energy equation becomes

$$\rho_l c_{p,l}(\vec{V} \cdot \nabla T) = k_l \nabla^2 T \tag{3}$$

The momentum and energy equation for the solid substrate maybe represented as

$$\vec{V} = 0 \tag{4}$$

Energy equation for heat conduction in solid substrate is given by

$$\frac{\partial}{\partial x}\left(k_s \frac{\partial T_w}{\partial x}\right) + \frac{\partial}{\partial y}\left(k_s \frac{\partial T_w}{\partial y}\right) + \frac{\partial}{\partial z}\left(k_s \frac{\partial T_w}{\partial z}\right) \tag{5}$$

In the above equations, V is velocity vector. p, k, T, ρ and c_p are respectively, pressure, thermal conductivity, temperature, density and specific heat. The subscript w, l and s represent the wall, liquid and solid respectively.

Temperature dependence of two important properties of water i.e. density and viscosity have been incorporated to ensure more accurate prediction of the results. These properties have been varied as per the following quadratic equations.

$$\rho_l = 758.1214 + 1.8761T - 3.604 \times 10^{-3}T^2 \tag{6}$$

$$\mu_l = 0.02143 - 1.195 \times 10^{-4}T + 1.699 \times 10^{-7}T^2 \tag{7}$$

Non-linear regression analysis has been done to obtain these polynomial quadratic equations. In the above equations ρ and μ are density and viscosity respectively. T is the temperature in kelvin.

2.2. Boundary conditions and numerical methodology

Proposed heat sinks are heated with uniform heat flux (q) at the bottom wall ($z = 0$). Whereas, remaining walls have adiabatic boundary condition ($q = 0$). At the inlet and outlet of the heat sink, velocity and pressure boundary conditions are applied respectively. Uniform velocity profile and inlet coolant temperature of $T_{in} = 303.15$ K has been considered at inlet. Simulations have been carried out for laminar flow since maximum value of Re is 500. At the outlet of the channel atmospheric pressure exists. No-slip condition was implemented at the walls of the channel. Commercially available software ANSYS FLUENT based on finite volume method (FVM) has been used in the present simulation. Momentum and energy equations have been discretized using second order upwind scheme. SIMLEC algorithm is used to solve the conjugate pressure-velocity coupling heat conduction and convection. Similar approach has been used in the literature [5,7] to solve such type of problems. Meshing of the computational domain has been accomplished through non-uniform grids of hexahedral and tetrahedral cells.

Grid independency test has been carried out to identify the optimum size of the mesh. Simulations have been performed for three different mesh sizes. Table 2 shows the mesh configuration of heat sink for fin height of 0.5 mm. Predicted numerical results from first two sets of grid are almost similar within the maximum difference of 1%. Hence, it was decided to simulate the problem with 275,092 numbers of nodes and 1,275,465 no. of elements for the 0.5 mm fin height heat sink. Similarly, for other cases also element size of $7e^{-5}$ has been considered. It is to be noted that with this mesh configuration, the convergence criteria for continuity and momentum equation was set to be 10^{-4} and for energy equation it was 10^{-6}. In the present operating range, convergence history of each configuration was very smooth however; with increasing Re computational complicacy of the problem may further increase. It is worth mentioning that heat sink of fin height 1 mm takes minimum computational time to reach the converge solution compared to shorter fin height.

Calculation of Re has been done on the basis of flow velocity and fluid properties at the entrance of inlet plenum of the heat sink. It may be expressed as

$$Re = \frac{\rho_l u_{in} D_h}{\mu_l} \tag{8}$$

in this expression ρ and μ are density and viscosity of water at the inlet of the heat sink respectively. Hydraulic diameter (D_h) has also been calculated at the entry of inlet plenum which can be expressed as

$$D_h = \frac{4A_c}{P} \tag{9}$$

where A_c and P are cross-sectional area and perimeter respectively at the inlet of heat sink. It should be noted that value of D_h remains same i.e. 1.56 mm for all the configurations of the heat sink. Average value of heat transfer coefficient has been calculated from the following expression.

$$\bar{h} = \frac{q \times A_b}{A_{conv}(\bar{T}_w - \bar{T}_l)} \tag{10}$$

In the above equation, q is the uniform heat flux applied at bottom; A_b footprint area of the microchannel heat sink. Footprint area remains same for all configurations of heat sink. $\bar{T}_w$ is the average bottom wall temperature and it has been estimated as area weighted temperature. $\bar{T}_l$ is the average temperature of inlet and outlet coolant. A_{conv} is actual convective area responsible for heat transfer. It should be noted that A_{conv} is a function of fin height (H_f) which has been calculated using the following expression.

$$A_{conv} = 79.5H_f + 82.5 \tag{11}$$

in the above equation, calculated values of A_{conv} is obtained in mm^2. Once the value of average heat transfer coefficient is calculated, average Nusselt Number ($N\bar{u}$) has been estimated from the following equation:

$$N\bar{u} = \frac{\bar{h} D_h}{k_l} \tag{12}$$

Table 2
Mesh configuration of 0.5 mm fin.

Element size (m)	No. of nodes	No. of elements
$6e^{-5}$	417,879	2,000,377
$7e^{-5}$	275,092	1,275,465
$8e^{-5}$	180,781	853,702

Table 3
Operating variable.

Re	Heat flux (q) kW/m^2	Fin height (H_f) mm
100–400	100–500	0.4–1.0

where k_l is the thermal conductivity of the coolant. Simulation work of total seven heat sink configurations has been accomplished using following variable parameters as shown in Table 3.

2.3. Validation of the model

In order to validate the present numerical model, research work of Qu and Mudawar [30] has been reproduced using the methodologies of the proposed model. Identical geometry i.e. single microchannel and same initial and boundary conditions have been imposed to predict the results. All external walls have been given adiabatic condition. Comparison of pressure drop data has been done at q = 100 W/cm^2, and for the *Re* values ranging from 100 to 800 at the increment of 100. Numerical assumption and simplification as mentioned in Section 2.1 have been used to simulate the problem. Fig. 2 conforms that present numerical model predicts pressure drop very close to the experimental findings. Pressure drop increases almost linearly with increasing *Re*. Using the present model, further comparison of temperature profile and Nusselt number (*Nu*) have also been done with another numerical results of the Qu and Mudawar [31] at *Re* 140 and q = 50 W/cm^2. It may be observed that results are in good agreement with the prediction of Qu and Mudawar [31] as shown in Figs. 3 and 4.

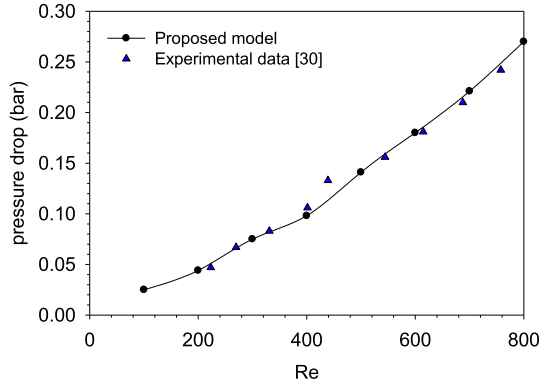

Fig. 2. Comparison of pressure drop with the experimental work of Qu and Mudawar [30].

Following observations may be drawn from the comparison of temperature profile and Nusselt number from the Figs. 3 and 4.

- Temperature gradient curves at the vertical middle plane of the channel clearly discriminates the solid substrate and liquid coolant zone due to the fact that the solid silicon has higher thermal conductivity causing less temperature gradient compared to fluid. Fig. 3 also illustrates that top wall of the channel is heated as temperature gradient exists from top to channel.
- *Nu* is notably high in the channel entrance region due to thermally developing length however; it becomes constant in the developed zone. In addition, compared to top wall, side walls exhibit overall high Nusselt number.

3. Results and discussion

3.1. Temperature profile

Numerical simulations were carried out and results have been compiled for four values of Reynolds numbers i.e. 100, 200, 300

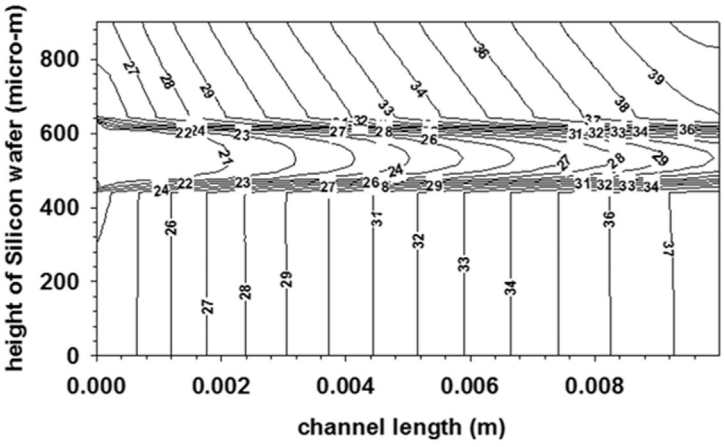

(a) Present results

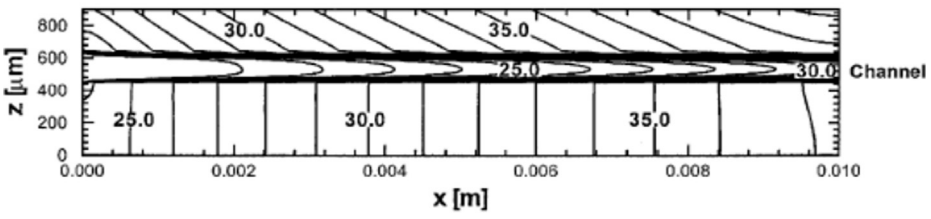

(b) Qu and Mudawar (2002) results

Fig. 3. Comparison of temperature profile at the middle plane of the channel with Qu and Mudawar [31].

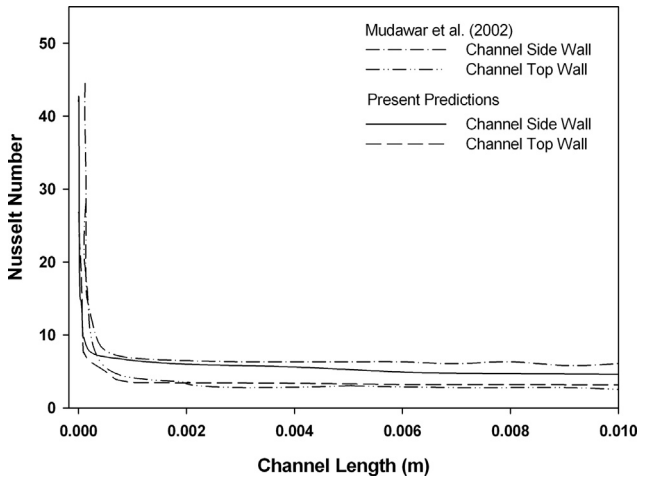

Fig. 4. Comparison of Nusselt number with Qu and Mudawar [31].

and 400, five values of heat fluxes (q) = 100, 200, 300, 400 and 500 kW/m^2 and all seven configurations (0.4–1.0 mm) of fin heights. Fig. 5 shows the average bottom wall temperature ($\bar{T}_w$) of all seven types of microchannel heat sinks for *Re* 200 and 300. It is worth mentioning that the value of $\bar{T}_w$ is the area weighted average temperature of the bottom wall surface. It can be anticipated that linear increase of $\bar{T}_w$ is due to higher heat input to the heat sink. Increasing trend of $\bar{T}_w$ is inevitably similar for all fin heights and Reynolds number. Nevertheless, slope of the curves decreases with increasing fin height (up to 0.8 mm) at higher heat fluxes. This clearly indicates that compared to shorter fins, bigger fins are able to dissipate more heat at higher heat fluxes and hence increasing rate of bottom wall temperature is controlled. Furthermore, significant difference in temperature value may be observed with varying fin height (H_f). As shown in Fig. 5(a), maximum value of $\bar{T}_w$ has been found for H_f = 0.4 mm at all ranges of applied heat fluxes. Higher average temperature of bottom wall is due to the fact that lesser amount of heat is being dissipated from the microchannel heat sink. However, increasing fin height beyond 0.4 mm, provides the lower value of $\bar{T}_w$, this may be attributed to higher heat transfer from the channel. Decreasing magnitude of $\bar{T}_w$ continues up to H_f = 0.8 mm. It is interesting to observe that beyond the fin height of 0.8 mm, decreasing tendency of $\bar{T}_w$ alters and at H_f = 0.9 mm it acquires almost equal values as of bottom wall temperature corresponding to 0.8 mm.

Both curves closely overlap for all values of heat fluxes. Overlapping of data for the fins of 0.8 and 0.9 mm stipulates the equivalent performance of both fins. Fundamentally, fin of 0.9 mm height consists of larger net convective area and hence, could have better heat transfer performance but supremacy of coolant flow behavior in 0.8 mm fin make this configuration more efficient. Further increasing the fin height to 1.0 mm results in higher average bottom wall temperature. It may be carefully observed that temperature curve of fin 1.0 mm overlaps the curve of H_f = 0.7 mm. It clearly indicates that completely closed heat sink of 1.0 mm fin height exhibits lower thermal performance which is even lesser than 0.9 and 0.8 mm fin heights. In Fig. 5(a) maximum value of $\bar{T}_w$ has been found to be 361.3 K at q = 500 kW/m^2 for the fin height of 0.4 mm whereas minimum is 339.6 K at the fin height of 0.8 mm. At the similar operating conditions $\bar{T}_w$ is 342.4 K for

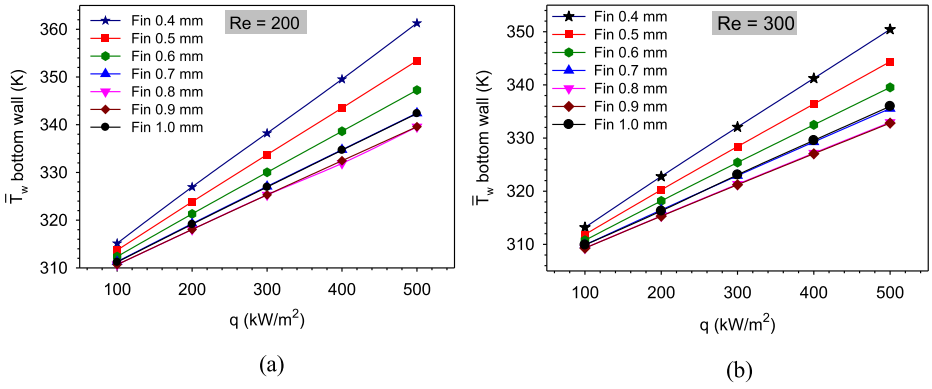

Fig. 5. Variation of average bottom wall temperature for different fin configurations.

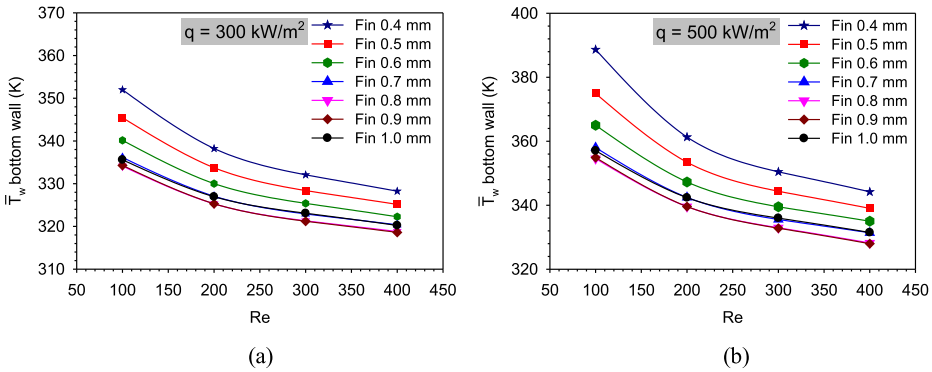

Fig. 6. Average bottom wall temperature for different fin configurations with *Re*.

H_f = 1.0 mm. Fig. 5(b) shows the $\bar{T}_w$ corresponding to Re = 300 with varying heat flux. As anticipated, at higher Re, overall temperature of bottom wall drops subsequently maximum and minimum reported average temperatures are 350.4 K and 332.9 K corresponding to fin heights of 0.4 mm and 0.8 mm respectively at q = 500 kW/m^2. It is important to note down that at Re = 300 also, minimum $\bar{T}_w$ has been reported for fin height of 0.8 and 0.9 mm since both line overlay each other. Above discussion concludes that compared to completely closed microchannel heat sink of fin height 1.0 mm, slightly smaller fin height provides the favorable coolant-solid surface interaction for better heat transfer. It is understood that in such case, top surface of the fins are also added in the actual convective area responsible for heat transfer consequently, whole convective surface area (A_{conv}) including fins, channels and side walls are fully submerged in the coolant that accelerates the heat transfer process.

Fig. 6(a & b) shows the effect of Reynolds number on bottom average temperature for different fin heights. As demonstrated in Fig. 6(a), increasing Re significantly reduces the $\bar{T}_w$ which is obvious because more heat is taken away by the coolant. Each curve of different fin height has similar slope which is quite steeper up to Re = 250 after that slope becomes moderate. Slopes of the curves are even steeper for the heat flux of q = 500 kW/m^2 as shown in Fig. 6(b). However, range of $\bar{T}_w$ increases by 5–10% which is higher for lowest fin height and continuously reduces with increasing fin height up to H_f = 0.8 mm. For this case also, $\bar{T}_w$ of bottom wall is consistently higher for the fin height of 1.0 mm and its values superimpose to fin of 0.7 mm.

3.2. Heat transfer coefficient

Fig. 7(a & b) shows the effect of heat flux on average heat transfer coefficient ($\bar{h}$) for different values of fin heights. Both plots corresponding to Re = 200 and 300 illustrate that irrespective of fin height, $\bar{h}$ increases almost linearly with q, although increase of $\bar{h}$ is very nominal. On the other hand, significant variation in $\bar{h}$ exists with changing fin heights. Minimum value of heat transfer coefficient has been found for shortest fin height of 0.4 mm which is lying between 4965 and 5103 W/m^2 K for all heat flux ranges at Re = 200. Similarly, at Re = 300 as shown in Fig. 7(b), values of $\bar{h}$ have been estimated in the range of 5757 to 6081 W/m^2 K for fin height 0.4 mm. Increasing fin height results in consistent increase of $\bar{h}$ with approximate margin of 500 W/m^2 K. Such growth tendency of $\bar{h}$ happens up to the fin of 0.8 mm where heat transfer coefficient is maximum for all values of heat fluxes. Reported values of $\bar{h}$ are 6907 W/m^{2}K and 7194 W/m^2 K respectively for q = 100 and 500 at Re = 200.

Further increase in H_f to 0.9 and 1.0 mm considerably reduces the $\bar{h}$. Additionally, heat transfer performance of the heat sink with 1.0 mm fin height degrades with increasing value of heat flux as shown in Fig. 7 (b) and approaches even lesser than the heat sink of 0.7 mm fin height. Quantitatively, conventional microchannel heat sink of fin height 1.0 mm shows the lesser heat transfer rate than fin height of 0.8 mm by 5–10%. Influence of Re on average heat transfer coefficient is notably high as shown in Fig. 8(a & b). It may be commonly observed that for fixed value of heat flux, growth

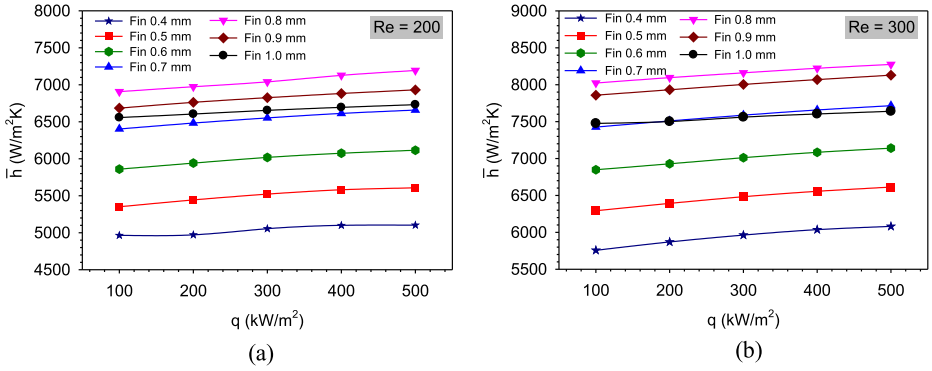

Fig. 7. Effect of fin height and heat flux on heat transfer coefficient.

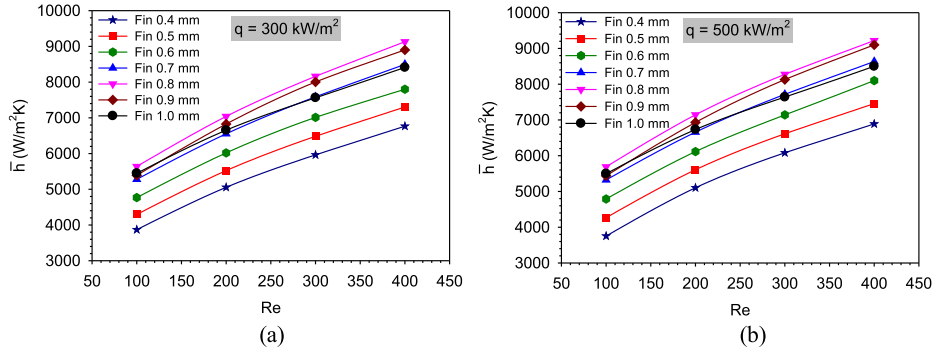

Fig. 8. Effect of fin height and Re on heat transfer coefficient.

rate of $\bar{h}$ is comparatively higher up to Re = 250 and after that slope of the curves slightly reduces for all values of fin heights.

Close observation of the curves corresponding to 0.9 and 1.0 mm fin heights reveal that although 0.9 mm fin is able to sustain the heat transfer performance (slightly lesser than 0.8 mm fin) with increasing Re, heat sink of 1.0 mm fin height continuously degrades the $\bar{h}$ at higher Re and slope of the curve evidently drops after Re = 250. Similar to $\bar{h}$, local heat transfer coefficient may also be calculated (using Eq. (10)) at any spatial location in the flow domain by taking the values of wall temperature and coolant temperature at that location. Higher values of local heat transfer coefficient may exist at the entrance region of the channel due to developing boundary layers. However, as flow progresses along the flow direction, its value reduces close to $\bar{h}$ and becomes stable in the downstream section of the channel.

Fig. 9 shows the average Nusselt No. ($N\bar{u}$) of all heat sink configurations with varying Re and for fixed value of heat flux. Similar to heat transfer coefficient, $N\bar{u}$ is also a strong function of Reynolds number irrespective of fin height. $N\bar{u}$ varies from 15 to 24 for fin height of 0.8 mm which is the maximum $N\bar{u}$ among all fin configurations. It indicates that fin height of 0.8 mm has the optimum heat dissipation capacity compared to remaining fin configurations in the present operating ranges.

It is interesting to observe that the microchannel heat sink with fin height of 0.9 mm holds the maximum actual convective area (A_{conv}) even then 0.8 mm fin shows the better heat transfer performance. This may be attributed to distinct flow behavior of the coolant which will be discussed in detail in the coming sections. In addition to facilitate higher heat transfer, fin height of 0.8 mm has also certain merits over completely closed heat sink (i) comparatively less material is required for fabrication attributes to lighter weight (ii) as it holds open space above fin top, uniform coolant distribution necessarily at the channel entrance is not a concern.

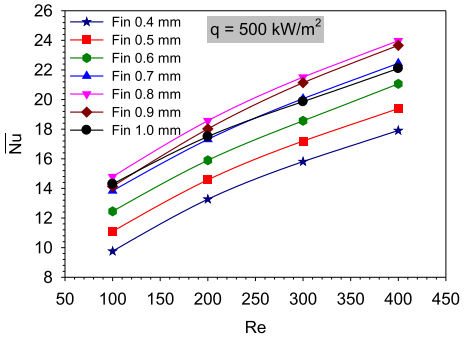

Fig. 9. Variation of average Nu with Re and fin height.

3.3. Temperature contour

Fig. 10 shows the temperature contour of the bottom wall for different fin heights at Re = 300 and q = 500 kW/m^2. Coolant flow direction is shown in the figure which is from left to right. Color configuration from blue to red represents the lower to higher temperature respectively. Contours of temperature distribution visibly differentiate the inlet plenum and channel sections of the microchannel heat sink. The pattern of temperature distribution in the inlet plenum of 0.4 mm fin resembles different compared to the remaining fin configurations.

It is due to the fact that more open space is available at the top in case of 0.4 mm fin which causes the through passage of significant amount of coolant from inlet plenum. Consequently, coolant crosses the entire flow path without efficient participation in the heat transfer process. This results in higher average temperature of the bottom wall of 0.4 mm fin height. Continuous increase in temperature can be observed along the flow direction of the coolant because temperature gradient between bulk fluid and solid substrate keeps on reducing. Temperature variation from 332 to 362 K has been found for the fin of 0.4 mm height.

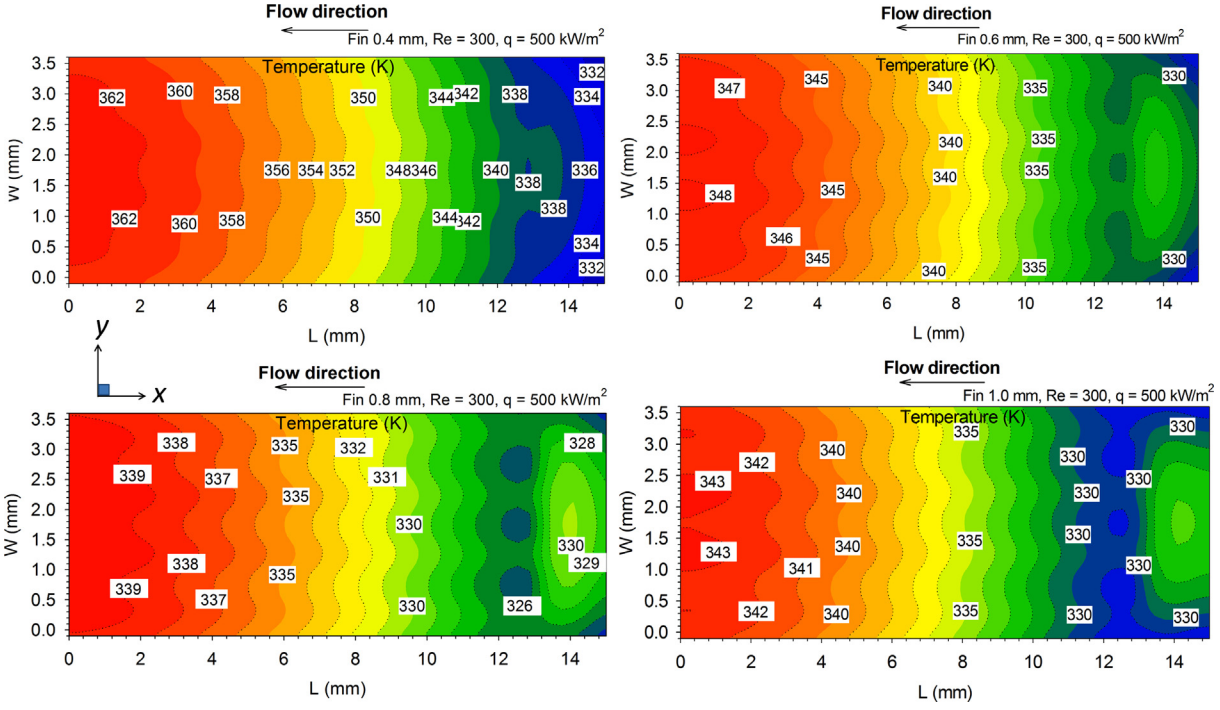

Fig. 10. Temperature contour of bottom wall for selected fin heights at Re = 300 and q = 500 kW/m^2.

Remaining three bottom walls of fin height 0.6 mm, 0.8 mm and 1.0 mm have almost similar pattern of temperature distribution. Unlike fin of 0.4 mm, it may be observed that a low temperature zone appears just after the inlet plenum. Low temperature zone is certainly due to sudden increase in velocity of the coolant at the microchannel inlet resulting, more heat carried out by liquid coolant from that location. Other portion of the bottom wall shows comparable temperature distribution except the magnitude of temperature. Among these four fins, average bottom wall temperature is minimum for 0.8 mm fin height heat sink and lie between 326 and 339 K. The range of temperature varies from 330 to 348 K for fin height 0.6 mm and 330 to 343 K for 1.0 mm fin height respectively.

Fig. 11 shows the temperature profile at the middle plane along the thickness of the heat sink corresponding to $Re = 300$ and $q = 500$ kW/m^2. It is important to point out that considered middle plane is at a distance of 0.5 mm from bottom wall hence, it is situated beyond the fin height of 0.4 mm and positioned at 0.1 mm above the top surface of fin (in the region of open space) that contains only fluid. This plane captures the fluid flowing very close to the fin top surface for 0.4 mm fin and hence, it can be seen that coolant has relatively more temperature which is clearly visible in the first contour plot. Moreover, it also confirms the establishment of thermal boundary layer adjacent to the top surface of the fin that can be better seen in the Fig. 12. Considered middle plane for remaining three heat sinks i.e. of fin 0.6 mm, 0.8 mm and 1.0 mm certainly captures both zones i.e. solid fin and liquid coolant. In Fig. 11, solid and fluid sections are clearly differentiable due to the fact that solid zone made of cooper has very high thermal conductivity compared to liquid coolant. Hence, significantly low temperature gradient exists in the substrate material whereas coolant has high temperature gradient. Moreover, temperature contour depicts that irrespective of fin height, temperature of the fin and bulk fluid increases along the flow direction. The overall temperature distribution reflects the lowest fin temperature for 0.8 mm fin followed by fin heights of 1.0 mm and 0.6 mm respectively.

Temperature distribution across the cross-section at a plane located at $x = 7.5$ mm (middle plane along channel length) from inlet has been shown in Fig. 12. Contours have been shown for fin heights of 0.4 mm, 0.8 mm, 0.9 mm and 1.0 mm at $Re = 200$ and $q = 400$ kW/m^2. Microchannel heat sink of fin height 0.4 mm holds considerably enough open space at the fin top through which mainstream volume of coolant flows. Such channel geometry and coolant flow behavior allows less interaction between solid surface and fluid, resulting reduced heat dissipation from this configuration. With increasing fin height, solid-fluid interaction or net convective area (A_{conv}) increases hence, heat transfer rate also increases. However, beyond 0.8 mm i.e. in microchannel of 0.9 mm fin height, flow of coolant confines in the channel with very less exposure to the open space, such flow characteristic no more supports to further enhance heat transfer. Resulting heat transfer enhancement stops and further reduces in 1.0 mm fin, since coolant flow is completely restricted to channel only.

3.4. Pressure profile

A comparative pressure drop in all fin configurations has been illustrated in the Fig. 13(a & b). In order to acquire the pressure drop along the flow direction a line has been drawn 0.2 mm above the channel bottom wall (at a location $y = 0.125$ mm from side wall and $z = 0.3$ mm from bottom). It can be seen in the Fig. 13(a) that pressure drop trend is almost similar for all heat sink configurations. However, significant variation in magnitude of pressure drop happens with minimum and maximum values of 103.3 Pa and 311.5 Pa respectively for 0.4 and 0.9 mm fin heights corresponding to $Re = 300$ and $q = 500$ kW/m^2. Fin configuration 1.0 mm compromises 290.4 Pa pressure drops which exist between pressure values of 0.8 and 0.9 mm fin height. Apparently, increasing fin height raised the flow obstruction causes pressure drop to increase. In addition to this, increasing fin height also increases the confinement of the open space which further contributes to raise pressure drop up to some extent. Higher value of pressure drop in 0.9 mm fin height compared to 1.0 mm fin is resulted due to this

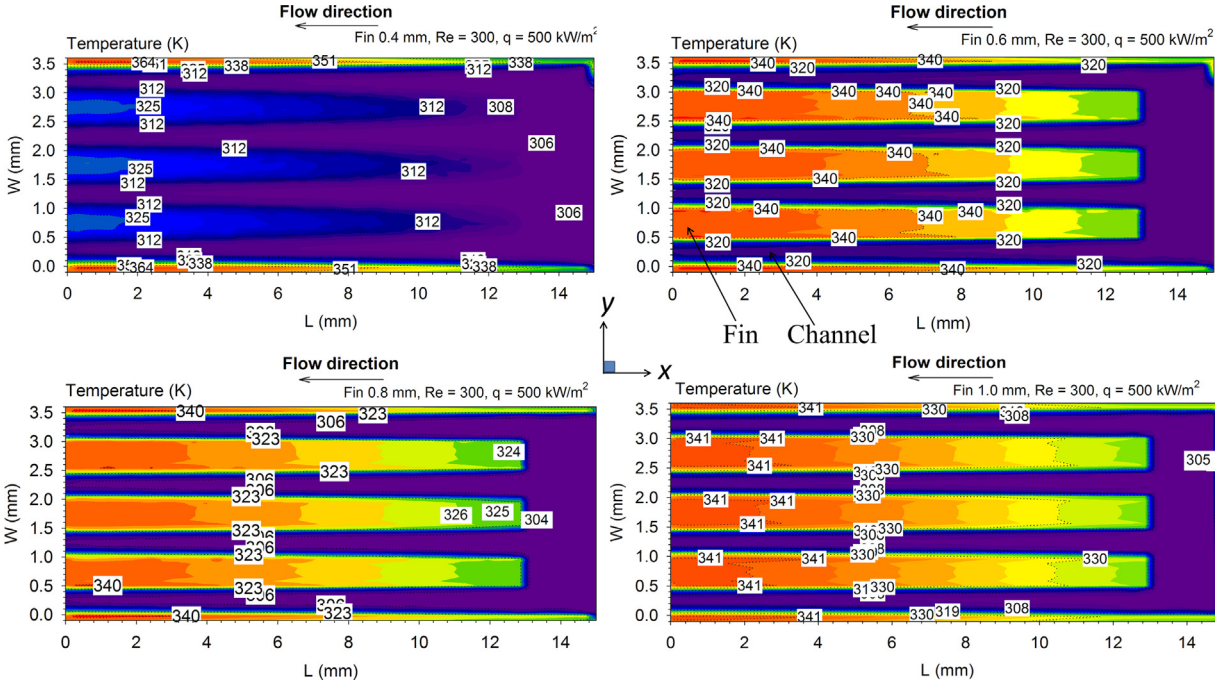

Fig. 11. Temperature contour at middle plane (at $z = 0.5$ mm from bottom) for selected fins at $Re = 300$ and $q = 500$ kW/m^2.

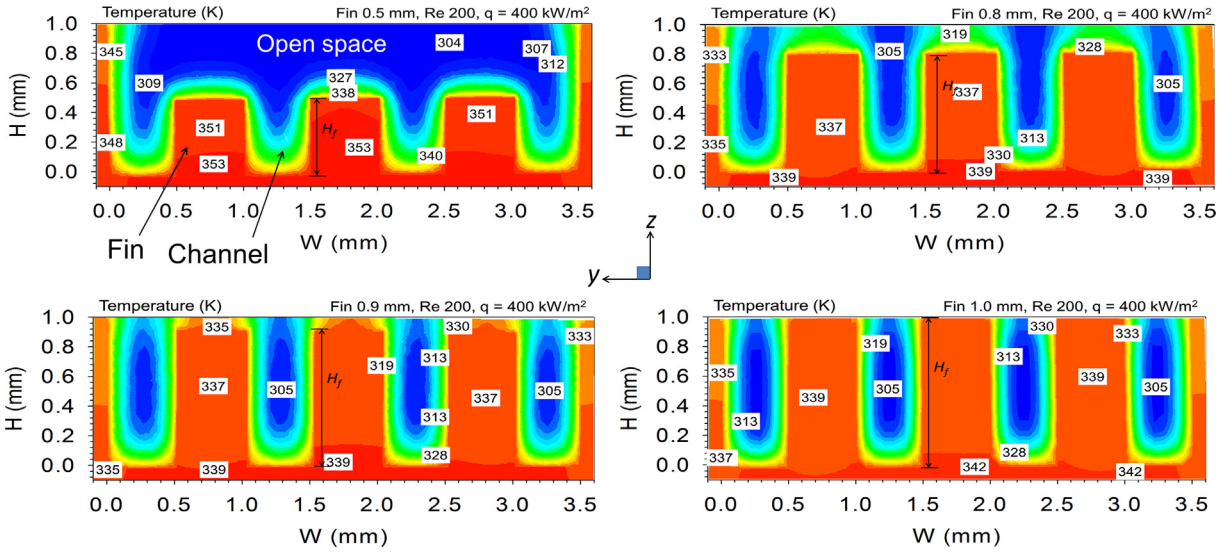

Fig. 12. Temperature contour across cross-section (at x = 7.5 mm from inlet) for selected fins at Re = 200 and q = 400 kW/m^2.

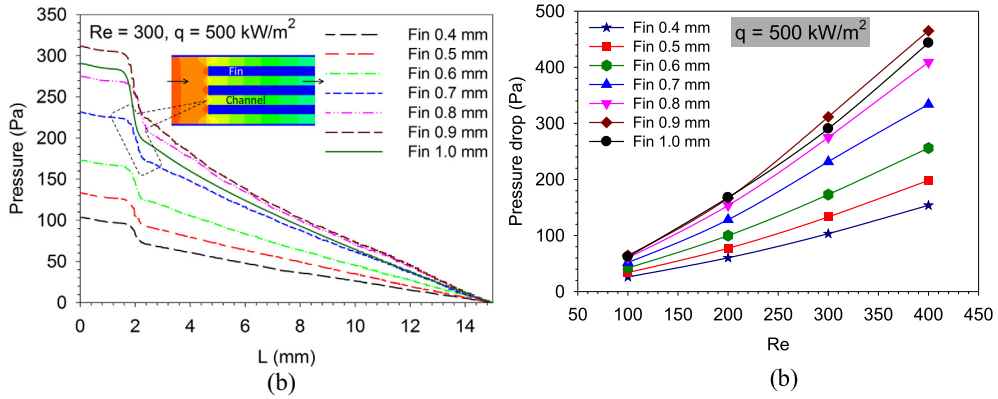

Fig. 13. (a) Pressure drop along the channel length and (b) Influence of Re and fin type on pressure drop.

confinement effect. In Fig. 13(a), all pressure curves witness sudden drop in pressure at a distance of 2 mm from inlet because at this location coolant is entering in the channels which is quite confined compared to inlet plenum. After that, merely linear pressure drop occurs. Fig. 13(b) illustrates the effect of Re on pressure drop for all fin heights at q = 500 kW/m^2. Two observations may be drawn from the plot i.e. pressure drop increase with Re for all curves which is certainly obvious. Nevertheless, it is interesting to note that slope of the curves are considerably high with increasing Re and fin height. The maximum value of pressure drop i.e. 465 Pa has been found for the fin height of 0.9 mm at the Reynolds number of 400. It may be conclude that higher Re would drastically raise the pumping power requirement of the microchannels.

Both plots of the pressure drop clearly demonstrate that heat sink of 0.8 mm fin height has reasonably less pressure drop compared to 0.9 mm and 1.0 mm fin heights. Hence, H_f = 0.8 mm can be a better choice in respect to pressure drop and high heat transfer. Moreover, influence of temperature on pressure drop has not been reported in the current operating range and parameters.

Fig. 14 exhibits the pressure contour at the middle plane along the thickness of the microchannel heat sink. Pressure distribution has been shown for the fin height of 0.8 mm at Re = 300 and q = 500 kW/m^2. Red and blue colors indicate higher and lower pressure zone respectively. In the contour plot, channel and fin segments are clearly identified, since pressure values (blue color)

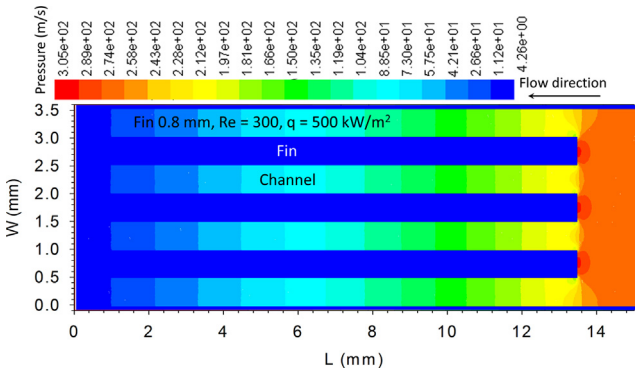

Fig. 14. Pressure contour at the middle plane (z = 0.5 mm from bottom) for 0.8 mm fin.

do not exist for the fin segments. It is obvious that pressure continuously reduces from inlet to outlet side. As discussed in the earlier section, it may be clearly observed that sudden pressure drop occurs at the inlet of the channels as coolant enters from inlet plenum to channel. Besides, some amount of the fluid hits the leading face of the fin and come to rest, consequently, high pressure location creates that can be seen in Fig. 14. Three high pressure spots are resulted due to this reason and appeared in the contour plot.

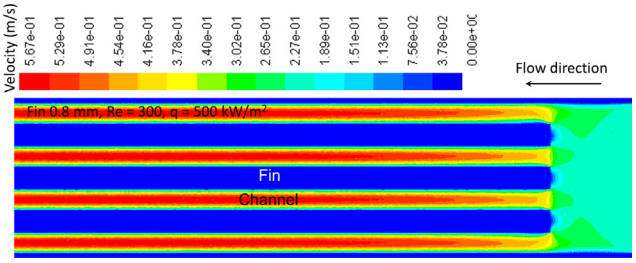

Fig. 15. Velocity contour at the middle plane (z = 0.5 mm from bottom) for 0.8 mm fin.

3.5. Flow characteristics

Flow behavior of the coolant has been illustrated through velocity contour as shown in Figs. 15 and 16. Fig. 15 represents the velocity profile at the same plane which has been considered in the earlier discussions. Coolant enters into the inlet plenum through uniform velocity and approaches to the inlet section of the channels. Coolant manages to enter smoothly in the two middle channels situated in-between the side channels. Whereas, in both the side channels it appears that certain amount of fluid is directed from the main stream in addition to direct access of the reasonable amount of the coolant as shown in Fig. 15.

Once fluid enters into the channel, it flows in a usual manner and flow gets fully developed after certain length. In order to better comprehend the flow nature, velocity contour has been shown across the cross-section of the heat sink in Fig. 16. Contour has been shown for fin heights of 0.4 and 0.8 mm articulating two different velocity profiles that have been explicitly reported in the present study. As shown in Fig. 16(a) when fin height is small enough such as 0.4 mm, mainstream coolant flow and hence development of velocity profile is centered in the available open space at the fin top. Therefore, contour of maximum velocity attains in that region only whereas channel depth is typically shielded with thick hydrodynamic boundary layer. Such characteristics of velocity evolution and existing contact surface have less potential to dissipate heat. Above discussion highlights two major causes of reduced heat transfer from this channel configuration (i) less convective surface area and (ii) concentrated bulk fluid flow behavior in the region which is least exposed to heating surface. However, as the fin height increases, two important phenomenon's happen simultaneously i.e. convective surface area increases and scattered flow behavior of the coolant emerges. Once the fin height is long enough, channels become the prominent passage for coolant flow as can be seen from the Fig. 16(b). Unlike smaller fin heights of Fig. 16(a), well-developed velocity profile appears in the channel for fin height of 0.8 mm. The maximum coolant velocity exists in the channel passage only, and scattered nature of the flow exists in the open space available at the fin top. The combined effect of such flow behavior of coolant, favors the heat transfer capacity of the heat sink. Consequently, microchannel heat sink of fin height 0.8 mm has got good potential to dissipate more heat compared to its remaining six counterparts.

Further increase of the fin height to 0.9 mm, although increases the net convective area nevertheless, coolant flow is extremely confined in the channel passage with very less exposure to the open space. Part of the heat that was carried out by coolant flow in the open space is reduced and heat sink behaves somewhat like completely closed channel. Therefore, heat transfer enhancement stops and further reduces in heat sink of 1.0 mm fin since; coolant flow is completely restricted to channel passage only. Above facts and discussion conform that in addition to net convective area, favorable fluid flow behavior caused by novel flow passages facilitates enhanced heat transfer. It is worth mentioning that heat sink of fin height 0.8 mm holds the merits of appropriate fin that provide reasonably adequate convective surface area along with optimum open space which enables coolant to carry out more heat. Partial confinement nature of the open space available at the top may propagates scattering flow behavior and thinner boundary layer resulting increased heat transfer in the heat sink of 0.8 mm fin compared to remaining configurations.

4. Conclusion

Influence of varying fin height on heat transfer and coolant flow behavior in rectangular parallel microchannels has been numerically studied. Seven different configurations of heat sink have been investigated for the *Re* range of 100–400 and heat flux range of 100–500 kW/m^2. Based on the comparative analysis of the results, following important findings have been reported.

- Increasing fin height, enables the heat transfer enhancement from the heat sink, however, beyond 0.8 mm of fin height, this trend no more persists. Further increase in fin height to 0.9 and 1.0 mm resulted in lesser heat transfer than 0.8 mm fin.
- Heat transfer rate drops by 5–10% in completely closed microchannel heat sink (of fin height 1.0 mm) compared to heat sink of 0.8 mm fin height. Available open space in this fin configuration facilitates favorable coolant flow passage to carry out more heat. Hence, it is desirable to slightly reduce the fin height (15–20%) to optimize the thermal performance.
- Pressure drop also rises with increasing fin height since longer fins create more obstruction in the flow path. Consequently, heat sinks of 0.4 mm and 0.9 mm fin height offer minimum and maximum pressure drop respectively.
- Magnitude of pressure drop in completely closed heat sink of 1.0 mm fin height is lying between 0.9 and 0.8 mm fin's heat sink with variation of ≈5–10%.

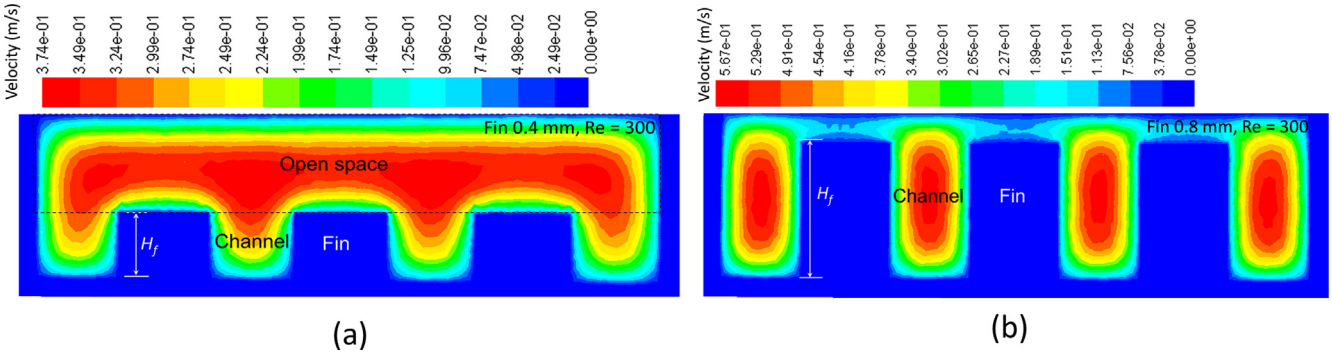

Fig. 16. Velocity contour across cross-section (at × = 7.5 mm from inlet) at *Re* = 300 and q = 500 kW/m^2.

- Open microchannel heat sinks hold additional merits over completely closed heat sink i.e. (i) comparatively less material is required attributes to lighter weight (ii) as it holds open space above fin top, uniform coolant distribution necessarily at the channel entrance is not a concern.

Conflict of interest

The authors declared that there is no conflict of interest.

Appendix A. Supplementary material

Supplementary data to this article can be found online at https://doi.org/10.1016/j.ijheatmasstransfer.2019.04.012.

References

[1] S. Kandlikar, History, advances, and challenges in liquid flow and flow boiling heat transfer in microchannels: a critical review, J. Heat Transfer 134 (2012), 034001-1–15.
[2] Y.K. Prajapati, P. Bhandari, Flow boiling instabilities in microchannels and their promising solutions – a review, Exp. Therm. Fluid Sci. 88 (2017) 576–593.
[3] P. Rosa, T.G. Karayiannis, M.W. Collins, Single-phase heat transfer in microchannels: the importance of scaling effects, Appl. Therm. Eng. 29 (2009) 3447–3468.
[4] W.M.A.A. Japar, N.A.C. Sidik, S.R. Aid, Y. Asako, T.L. Ken, A comprehensive review on numerical and experimental study of nanofluid performance in microchannel heat sink (MCHS), J. Adv. Res. Fluid Mech. Therm. Sci. 45 (2018) 165–176.
[5] H. Wang, Z. Chen, J. Gao, Influence of geometric parameters on flow and heat transfer performance of micro-channel heat sinks, Appl. Therm. Eng. 107 (2016) 870–879.
[6] G. Lu, J. Zhao, L. Lin, X.D. Wang, W.M. Yan, A new scheme for reducing pressure drop and thermal resistance simultaneously in microchannel heat sinks with wavy porous fins, Int. J. Heat Mass Transfer 111 (2017) 1071–1078.
[7] Y.F. Li, G.D. Xia, D.D. Ma, Y.T. Jia, J. Wang, Characteristics of laminar flow and heat transfer in microchannel heat sink with triangular cavities and rectangular ribs, Int. J. Heat Mass Transfer 98 (2016) 17–28.
[8] S.W. Beng, W.M.A.A. Japar, Numerical analysis of heat and fluid flow in microchannel heat sink with triangular cavities, J. Adv. Res. Fluid Mech. Therm. Sci. 34 (1) (2017) 1–8.
[9] Y.J. Lee, P.S. Lee, S.K. Chou, Enhanced thermal transport in microchannel using oblique fins, J. Heat Transfer 123 (2012), 101901-1–10.
[10] Y.J. Lee, P.K. Singh, P.S. Lee, Fluid flow and heat transfer investigations on enhanced microchannel heat sink using oblique fins with parametric study, Int. J. Heat Mass Transfer 81 (2015) 325–336.
[11] Y.K. Prajapati, M. Pathak, M.K. Khan, A comparative study of flow boiling heat transfer in three different configurations of microchannels, Int. J. Heat Mass Transfer 85 (2015) 711–722.
[12] Y.K. Prajapati, M. Pathak, M.K. Khan, Numerical investigation of subcooled flow boiling in segmented finned microchannels, Int. Commun. Heat Mass Transfer 86 (2017) 215–221.
[13] Y. Sui, C.J. Teo, P.S. Lee, Y.T. Chew, C. Shu, Fluid flow and heat transfer in wavy microchannels, Int. J. Heat Mass Transfer 53 (2010) 2760–2772.
[14] C.M. Karale, S.S. Bhagwat, V.V. Ranade, Flow and heat transfer in serpentine channels, AIChE J. 59 (2013) 1814–1827.
[15] I.A. Ghani, N. Kamaruzaman, N.A.C. Sidik, Heat transfer augmentation in a microchannel heat sink with sinusoidal cavities and rectangular ribs, Int. J. Heat Mass Transfer 108 (2017) 1969–1981.
[16] I.A. Ghani, N.A.C. Sidik, R. Mamat, G. Najafi, T.L. Ken, Y. Asako, W.M.A.A. Japar, Heat transfer enhancement in microchannel heat sink using hybrid technique of ribs and secondary channels, Int. J. Heat Mass Transfer 114 (2017) 640–655.
[17] X. Huang, W. Yang, T. Ming, W. Shen, X. Yu, Heat transfer enhancement on a microchannel heat sink with impinging jets and dimples, Int. J. Heat Mass Transfer 112 (2017) 113–124.
[18] L. Chai, G.D. Xia, H.S. Wang, Parametric study on thermal and hydraulic characteristics of laminar flow in microchannel heat sink with fan-shaped ribs on sidewalls – Part 1: heat transfer, Int. J. Heat Mass Transfer 97 (2016) 1069–1080.
[19] L. Chai, G.D. Xia, H.S. Wang, Numerical study of laminar flow and heat transfer in microchannel heat sink with offset ribs on sidewalls, Appl. Therm. Eng. 92 (2016) 32–41.
[20] S. Huang, J. Zhao, L. Gong, X. Duan, Thermal performance and structure optimization for slotted microchannel heat sink, Appl. Therm. Eng. 115 (2017) 1266–1276.
[21] T. Yeom, T. Simon, T. Zhang, M. Zhang, M. North, T. Cui, Enhanced heat transfer of heat sink channels with micro pin fin roughened walls, Int. J. Heat Mass Transfer 92 (2016) 617–627.
[22] D. Yang, Y. Wang, G. Ding, Z. Jin, J. Zhao, G. Wang, Numerical and experimental analysis of cooling performance of single-phase array microchannel heat sinks with different pin-fin configurations, Appl. Therm. Eng. 112 (2017) 1547–1556.
[23] V. Yadav, K. Baghel, R. Kumar, S.T. Kadam, Numerical investigation of heat transfer in extended surface Microchannels, Int. J. Heat Mass Transfer 93 (2016) 612–622.
[24] J. Zhao, S. Huang, L. Gong, Z. Huang, Numerical study and optimizing on micro square pin-fin heat sink for electronic cooling, Appl. Therm. Eng. 93 (2016) 1347–1359.
[25] E. Rasouli, C. Naderi, V. Narayanan, Pitch and aspect ratio effects on single-phase heat transfer through microscale pin fin heat sinks, Int. J. Heat Mass Transfer 118 (2018) 416–428.
[26] H.C. Chiu, R.H. Hsieh, K. Wang, J.H. Jang, C.R. Yu, The heat transfer characteristics of liquid cooling heat sink with micro pin fins, Int. Commun. Heat Mass Transfer 86 (2017) 174–180.
[27] J. Yang, L. Li, L. Yang, J. Li, Uniform design for the parameters optimization of pin-fins channel heat sink, Appl. Therm. Eng. 120 (2017) 289–297.
[28] Y. Zhai, G. Xia, Z. Li, H. Wang, Experimental investigation and empirical correlations of single and laminar convective heat transfer in microchannel heat sinks, Exp. Therm. Fluid Sci. 83 (2017) 207–214.
[29] I.A. Ghani, N.A.C. Sidik, N. Kamaruzaman, Hydrothermal performance of microchannel heat sink: The effect of channel design, Int. J. Heat Mass Transfer 107 (2017) 21–44.
[30] W. Qu, I. Mudawar, Experimental and numerical study of pressure drop and heat transfer in a single-phase micro-channel heat sink, Int. J. Heat Mass Transfer 45 (2002) 2549–2565.
[31] W. Qu, I. Mudawar, Analysis of three-dimensional heat transfer in micro-channel heat sinks, Int. J. Heat Mass Transfer 45 (2002) 3973–3985.